SOVIET PHYSICS

JETP

A translation of the Zhurnal Éksperimental'noĭ i Teoreticheskoĭ Fiziki

Vol. 22, No. 4, pp. 701-947 (Russ. Orig. Vol. 49, No. 4, pp 1009-1374, October 1965) April, 1966

INVESTIGATION OF THE OSCILLATIONS OF THE ABSORPTION COEFFICIENT OF SOUND IN BISMUTH. I. GEOMETRICAL RESONANCE

A. P. KOROLYUK

Radiophysics and Electronics Institute, Academy of Sciences, Ukrainian S.S.R.

Submitted to JETP editor March 25, 1965

J. Exptl. Theoret. Phys. (U.S.S.R.) 49, 1009-1018 (October, 1965)

Detailed investigations were carried out of the oscillations of the coefficient of absorption of sound in bismuth single crystals at the longitudinal vibration frequency of 500 Mc and 1.4°K. The three principal crystallographic planes were investigated. The form of the Fermi surface of bismuth is discussed on the basis of the results obtained.

1. INTRODUCTION

A considerable number of experimental and theoretical investigations have dealt with the Fermi surface of bismuth. The electron structure of bismuth has been investigated experimentally in greatest detail using the de Haas-van Alphen effect,[1-3] the Shubnikov-de Haas effect,[4] and the cyclotron resonance of this metal.[5-10] The oscillations of the absorption of ultrasound, mainly of the quantum type, were investigated by Reneker,[3] but his data were insufficient to determine the main dimensions of the Fermi surface, which are of considerable interest in view of the recent theoretical papers on the electron spectrum of bismuth.[11-14]

The investigations carried out so far have shown that the Fermi surface could be represented, in the first approximation, by one hole and three electron ellipsoids. According to the Jones-Shoenberg model, the electron ellipsoids are strongly elongated along one of the axes and located in such a way that the shortest axis coincides with the direction of a twofold symmetry axis, and the longest axis is inclined at an angle $\xi = 6°$ to the basal plane.

The hole ellipsoid is a surface of revolution about the trigonal axis of the crystal, along which the surface is elongated.

Since all the experiments on the quantum oscillations of various physical quantities have yielded data only on the areas of the cross sections of the Fermi surface, it seemed interesting to use the geometrical resonance method to make a direct determination of the extremal diameters of the bismuth Fermi surface.

In the present investigation, measurements were made, at 1.4°K, of the anisotropy of the oscillation periods in the geometrical resonance at a longitudinal acoustic frequency of 500 Mc, in a magnetic field of 10—2500 Oe.

2. METHOD OF MEASUREMENT

The measurements of the oscillation periods of the absorption coefficient were carried out using

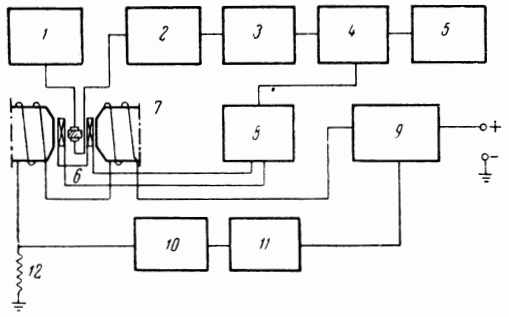

FIG. 1. Block diagram of the apparatus used in the measurements: 1) G-4-31 oscillator; 2) superheterodyne receiver; 3) low-frequency amplifier; 4) phase-sensitive detector; 5) ÉPP-09 automatic recorder; 6) investigated sample; 7) electromagnet; 8) unit for modulation of magnetic field; 9) electronic rheostat; 10) control voltage unit; 11) dc amplifier; 12) standard resistor.

an ultrasonic spectrometer working continuously. The apparatus (block diagram in Fig. 1) was similar to that used in Reneker's work [3] and differed from it only in the system for displaying the magnetic field and in special measures taken to screen the receiver from stray induced emf's originating from the oscillator.

The low-temperature part of the apparatus (the cryostat) was described in [15]; it was not modified in any essential respect.

A standard signal oscillator 1, type G-4-31, was used as the source of high-frequency oscillations. To reduce the ac noise, storage batteries were used to heat the filament of the oscillator tube. Piezoelectric quartz plates, of the X-cut and having a natural resonance frequency of about 100 Mc, were used as the transducers for converting the electromagnetic into ultrasonic oscillations.

The quartz plates were excited at the fifth harmonic. The signal transmitted through the sample 6 was picked-up by a high-sensitive superheterodyne receiver 2, amplified by a low-frequency amplifier 3, detected with a phase-sensitive detector 4, and recorded by an automatic recorder type ÉPP-09 (5 in Fig. 1) on an instrument chart.

Since the oscillations of the absorption coefficient were equidistant when plotted against the reciprocal of the magnetic field H, they were recorded using a hyperbolic time scale for the field, in order to make the analysis easier. The following system was used to control the electromagnet current: a control unit 10, a dc amplifier with a low zero drift 11, and an electronic rheostat 9. The correct linear scale for the reciprocal of the field was obtained by compensating the residual field of the electromagnet with a winding carrying a reverse current, so that H = 0 for J = 0.

The hyperbolic time scale in scanning made it possible to use the ÉPP-09 recorder without modification. With the application of a weak modulation signal of 50 cps frequency to a slowly varying main field, we recorded a quantity proportional to the derivative of the absorption coefficient with respect to the magnetic field: $d\Gamma/dH$. The time taken to record a single curve was 4—5 min.

The samples, in the form of disks about 2.5 mm thick and 8—10 mm in diameter, were cut by electro-spark machining from larger bismuth crystals grown in glass ampoules from grade V-000 metal. Subsequent gentle grinding of the ends with fine abrasives ensured the necessary plane-parallel form of the plates. The ratio of the resistances at room and helium temperatures R(300°)/R(4.2°), which represented the metal purity, ranged within the limits 90—120. The directions of the crystallographic axes were determined, using an optical goniometer, to within about 1°.

Since the mean free path of carriers in samples of this purity was not very high and, moreover, the magnitude of the oscillatory effect (extremely weak in bismuth due to the small number of electrons) was proportional to the square of the frequency, [16,17] it was necessary to use the highest possible sonic frequencies. However, the signal level decreased as the frequency increased, due to a reduction in the conversion factor and an increase in the absorption with frequency. Therefore, in practice, it was not possible to increase the frequency beyond 500 Mc. At this frequency, the ratio of the mean free path to the acoustic wavelength reached 30, so that we could observe reliably 6—10 oscillations of the absorption coefficient.

In our experiments, the magnetic field vector **H** was always orthogonal to the acoustic wave vector **K**. From the measured periods of the oscillations, we determined the extremal dimension $D_{ext} = |p_1 - p_2|_{ext}$ of the Fermi surface along the $\mathbf{K} \times \mathbf{H}$ direction using V. L. Gurevich's formula: [16]

$$D_{ext} = e\lambda / c\Delta H^{-1}$$

(e is the electronic charge, c is the velocity of light, and λ is the acoustic wavelength).

3. RESULTS OF MEASUREMENTS

The measurements of the oscillation periods were carried out for three orientations of the crystal with respect to the acoustic wave vector **K** and the magnetic field direction:

1. The wave vector was parallel to the binary

axis, and the magnetic field vector rotated in the plane of the trigonal and bisectrix axes. Such a geometry made it possible to obtain the projection of the extremal diameters of the Fermi surface on the plane of the trigonal and bisectrix axes ($\psi' = \varphi' + 90°$ was the angle between the trigonal axis and the magnetic field direction, φ' was the angle between the trigonal axis and the direction of the corresponding projection).

2. The wave vector was parallel to the trigonal axis and the magnetic field vector rotated in the plane of the binary axes. Using this orientation, we measured the projection of the extremal diameters of the Fermi surface onto the plane of the binary axes ($\psi'' = \varphi'' + 90°$ was the angle between a binary axis and the magnetic field).

3. The wave vector was parallel to the bisectrix axis. In this case, we measured the projection of the extremal diameters on the plane of the binary and trigonal axes ($\psi''' = \varphi''' + 90°$ was the angle between the trigonal axis and the magnetic field).

Typical dependences of the derivative of the absorption coefficient, $d\Gamma/dH$, are plotted in Fig. 2 as a function of the reciprocal of the magnetic field. The analysis of the curves and the determination of the oscillation periods presented, in most cases, no great difficulty and could be carried out graphically, especially if the frequency difference was great. In more complex cases, we could use the anisotropy of the values of the periods, recording the angular dependence every 1—0.5°, and then selecting for analysis those curves which exhibited clearly the integral-multiple ratio of the frequencies. The harmonic analysis was thus considerably simplified.

Figure 3 shows a record of $d\Gamma/dH$ as a function of the field for the second orientation of the crystal. The oscillations in weak fields (approximately up to

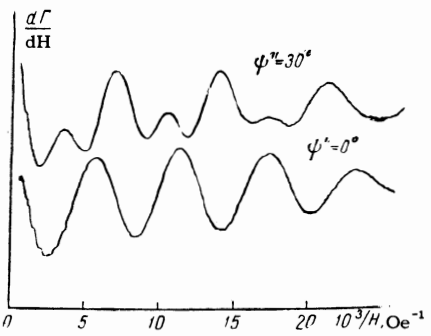

FIG. 2. Typical dependences of the derivative of the absorption coefficient $d\Gamma/dH$ on the reciprocal of the magnetic field for bismuth. The wave vector is oriented along the trigonal axis, $\nu = 508$ Mc, $T = 1.4°K$, ψ'' is the angle between a binary axis and the direction of the magnetic field in the plane of the binary axes.

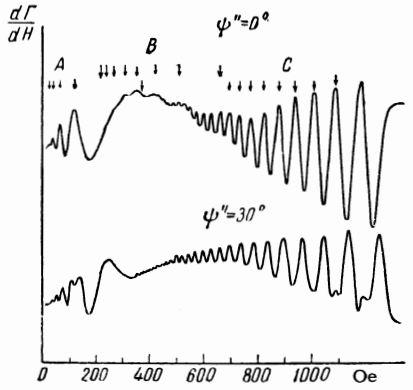

FIG. 3. Recording the derivative of the absorption coefficient plotted as a function of the field. Arrows A and B indicate the geometrical resonance, C indicates the quantum oscillations. The wave vector is oriented along the trigonal axis, $\nu = 508$ Mc, $T = 1.4°K$, ψ'' is the angle between a binary axis and the direction of the magnetic field in the plane of the binary axes.

500 Oe) represented the geometrical resonance, but in stronger fields they were the quantum oscillations of the absorption of sound. In the weakest field and with $\psi'' = 0$, the lines denoted by the arrows A in Fig. 3, originated from the two electron surfaces and had identical periods. The B lines were due to the third electron surface and their period governed the projection of the maximum dimension of the ellipsoid along a normal to the binary axis of the crystal. The quantum oscillations had only a single period in weak fields; the second period, corresponding to the larger cross section, was not observed in this range of fields, owing to the smallness of the oscillation amplitude. Since the periods of the geometrical and quantum oscillations originating from two electron surfaces were respectively identical, the dimensions and the areas of the cross sections of these surfaces were the same for $\psi'' = 0$. On going over to the angle $\psi'' = 30°$, the resultant curve represented the superposition of two components with periods differing by a factor of 2; consequently, for this direction of the field, the extremal dimensions and the areas of the cross sections of the surfaces differed by a factor of 2.

The same curves, but recorded as functions of the reciprocal of the magnetic field, are shown in Fig. 2. The quantum oscillations are practically invisible in them because of the rapid magnetic field sweep and the large time constant of the detector.

Figures 4—6 show the polar diagrams of the projections of the extremal dimensions of the Fermi surfaces onto the investigated crystallographic planes; the binary, bisectrix, and trigonal

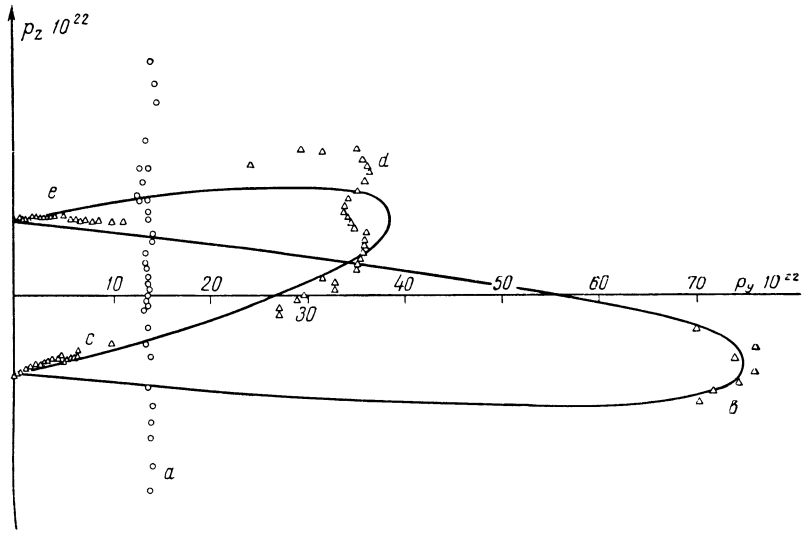

FIG. 4. Projection of the Fermi surfaces of bismuth onto the plane of the trigonal and bisectrix axes.

axes of the crystal are denoted by x, y, and z, respectively. The directions along which the experimental points in the diagrams were plotted, made 90° with the corresponding magnetic field orientation, which represented the direction of the measured extremal momentum along the crystallographic axes.

The oscillations denoted by a in Fig. 4 were due to holes, while the remaining four groups of points (b, c, d, e) were due to electrons. The investigated effect did not allow us to determine unambiguously the sign of the charge of the carriers responsible for the oscillations, but an investigation of the anisotropy of the periods and a comparison of the results obtained with those expected for the ellipsoid model of the surface helped one to make a sufficiently reliable analysis of the results. The continuous lines in these figures represent the projections of the electron ellipsoids onto the corresponding planes.

The oscillations b and e were due to the same ellipsoid, and the oscillation group b was observed most clearly at the angle $\psi' = -6°$. This corresponded to an inclination of the long axis of the ellipsoid of $\xi = 6°$ to the bisectrix. From the value of the minimum period of this group, we determined the dimension of the long semiaxis of the ellipsoid $p_2 = (76 \pm 3) \times 10^{-22}$ g-cm-sec^{-1} (the coordinate system associated with the ellipsoid is denoted by the subscripts 1, 2, 3). [1)]

Over a wide range of angles, the oscillations due to this ellipsoid were so weak that it was practically impossible to measure their periods. Only at $\psi' = 50°$ did we observe the oscillations e which were due to this ellipsoid and which governed its average dimension.

The oscillations d and c were associated with the two other ellipsoids, rotated in the plane xy by 120 and 240°. The periods, and consequently the projections of the extremal diameters of these surfaces onto the zy plane, were equal. Some deviation of the experimental points of group d from the convex ellipsoid projection was probably due to the slightly inaccurate alignment of the

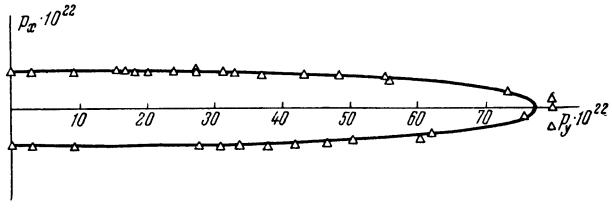

FIG. 5. Projection of the electron ellipsoid onto the plane of the binary axes.

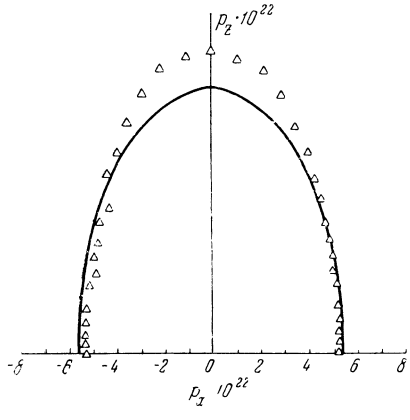

FIG. 6. Projection of the electron ellipsoid onto the plane of the binary and trigonal axes.

[1)]From now on, we shall take the momenta to have the dimensions g-cm-sec^{-1} and the areas to have the dimensions g^2 cm^2 sec^{-2}.

binary axis of the crystal with respect to the plane in which the magnetic field was rotated. From the angle $\Delta\psi'$, formed by the directions of the relative maxima of the points, we could estimate the error in the orientation of the sample: $\Delta\vartheta \approx \Delta\psi'/2\sqrt{3} \approx 2.5°$. The error $\Delta\xi$ in the determination of the angle ξ, due to the inaccurate alignment of the binary axis of the crystal, was small and could be ignored: $\Delta\xi = \xi(1 - \cos\Delta\vartheta')$.

The hole oscillations had considerable amplitude in the angular range $\psi = \pm 60°$, and they made it possible to determine the minimum dimension of the hole surface $p_h = (13.8 \pm 0.5) \times 10^{-22}$. Unfortunately, their amplitude near the angles $\psi' = 90°$ was so small that we were unable to determine their period with reasonable accuracy.

Figure 5 shows the results of the investigation of the second orientation of the crystal. In this plane, the oscillations of all three ellipsoids were clearly visible and the 60° symmetry of the periods was clearly evident, which made it possible to determine accurately, from the experimental points, the projection of one of the ellipsoids onto the plane of the binary axes. The other two ellipsoids gave exactly the same projections, except that they were rotated by 120 and 240°.

From the same diagram, we determined the shortest ellipsoid axis $p_1 = (5.5 \pm 0.2) \times 10^{-22}$. The oscillations of the hole surface for this orientation were weak and were observed only for some directions of the magnetic field.

The projection of the longest axis of the ellipsoid onto the same plane, determined from the minimum period at $\psi'' = 0°$, was in good agreement with the projection measured using the first orientation.

Figure 6 shows the polar diagram for the third orientation. In this plane, the hole oscillations and the oscillations of the two other ellipsoids were very weak and are not given in the figure. The oscillations of the ellipsoid elongated along the y axis were clearly visible and were measured with sufficient accuracy. The experimentally determined dimension of the projection along the z axis was found to be somewhat larger than the calculated value. This difference could also be explained by a slight misalignment of the crystal. The magnitude of this misalignment could be determined from the difference: $\sin\Delta\vartheta''' \approx \Delta\vartheta''' \approx \Delta p_z/p_2 \approx 1/76 \approx 0.75°$.

The dimension of the ellipsoid along the binary axis, obtained for the same orientation of the crystal, was also in good agreement with the measurements in other planes.

The velocity of longitudinal sound in bismuth s_l was anisotropic and the values used in the calculations were:

Trigonal axis: $s_l = 2.02 \times 10^5$ cm/sec

Binary axis: $s_l = 2.62 \times 10^5$ cm/sec

Bisectrix axis: $s_l = 2.70 \times 10^5$ cm/sec.

Strictly speaking, longitudinal waves could not be propagated along the bisectrix axis, but the longitudinal component in the excited modes was sufficiently strong to obtain signals of the required magnitude.

4. DISCUSSION OF RESULTS

We shall now list our experimental results, which are independent of any electron spectrum model.

1. The minimum value of the electron momentum is $p_1 = (5.5 \pm 0.2) \times 10^{-22}$. The direction of p_1 is along a binary axis of the crystal. The value and the direction of this momentum are in good agreement with $p_1 = (5.4 \pm 0.1) \times 10^{-22}$, obtained by Khaĭkin et al.[7] from sections of cyclotron orbits.

2. The maximum value of the electron momentum is $p_2 = (76 \pm 3) \times 10^{-22}$. The direction along which p_2 is greatest makes the angle $\xi = 6 \pm 1°$ with the bisectrix axis, in the plane of the bisectrix and trigonal axes.

3. The minimum value of the electron momentum in the plane of the bisectrix and trigonal axes is $p_3 = (7.6 \pm 0.3) \times 10^{-22}$. The exact direction of p_3 in this plane is difficult to determine because of the very broad maximum of the oscillation period near the angles $\psi' = 90°$; moreover, the determination is difficult because the periods for this and the other two surfaces are all approximately equal.

4. The value of the minimum momentum along the bisectrix axis is $p_h = (13.8 \pm 0.5) \times 10^{-22}$. This momentum is evidently due to the hole surface.

We shall now compare these results with the available models of the spectrum.

Quadratic approximation. In this case, the dispersion law for the energy of electrons in bismuth may be written as follows

$$\varepsilon = \frac{1}{2m_0}(\mathbf{p}\alpha\mathbf{p}). \tag{1}$$

Here m_0 is the free-electron mass; α is the reciprocal mass tensor, with the matrix written in terms of the crystal axes,

$$\|\alpha\| = \begin{Vmatrix} \alpha_{xx} & 0 & 0 \\ 0 & \alpha_{yy} & \alpha_{yz} \\ 0 & \alpha_{zy} & \alpha_{zz} \end{Vmatrix}. \tag{2}$$

The constant-energy surfaces are triaxial ellipsoids, the symmetry of the crystal permitting the rotation of the ellipsoids in the yz plane. We shall

represent the direction of the magnetic field in the crystal by the unit vector $\mathbf{n} = \mathbf{H}/|\mathbf{H}|$, and the direction of the propagation of sound by the unit vector $\mathbf{k} = \mathbf{K}/|\mathbf{K}|$, where the vectors $\mathbf{n}$ and $\mathbf{k}$ are orthogonal: $\mathbf{nk} = 0$.

In this case, we can easily obtain the formula for the projection of the extremal diameters of the ellipsoids for $\epsilon = \epsilon_f$ onto the plane $k \cdot p = 0$. This formula is

$$D_{ext} = \left[\frac{8m_0\varepsilon_f(\mathbf{k}\alpha\mathbf{k})}{\det\alpha(\mathbf{n}\alpha^{-1}\mathbf{n})}\right]^{1/2}, \qquad (3)$$

where α^{-1} is the reciprocal of the tensor α (the mass tensor).

For suitably selected directions of $\mathbf{n}$ and $\mathbf{k}$, this formula makes it possible to obtain most directly the values of α_{ik} from the measurement of the oscillation periods of the geometrical resonance in Fermi energy units ϵ_f. For example, if $\mathbf{k} = (0, 0, 1)$, $\mathbf{n} = (\sin\psi'', \cos\psi'', 0)$, Eq. (3) assumes the form

$$D_{ext} = \left[\frac{8m_0\varepsilon_f}{\alpha_{xx}\cos^2\varphi'' + (\alpha_{yy} - \alpha_{yz}^2/\alpha_{zz})\sin^2\varphi''}\right]^{1/2}, \qquad (4)$$

where $\varphi'' = \psi'' - 90°$, is the angle with respect to a binary axis in the plane of the binary axes. Thus, the oscillation period for $\psi'' = 90°$ makes it possible to determine the value of α_{xx} directly.

In the case $\mathbf{k} = (1, 0, 0)$, $\mathbf{n} = (0, \cos\psi', \sin\psi')$, we obtain the projection of one of the ellipsoids onto the yz plane:

$$D_{ext} = \left(\frac{8m_0\varepsilon_f}{\alpha_{yy}\sin^2\varphi' + \alpha_{zz}\cos^2\varphi' + \alpha_{yz}\sin 2\varphi'}\right)^{1/2} = \left(\frac{8m_0\varepsilon_f}{\alpha_2\sin^2\vartheta + \alpha_3\cos^2\vartheta}\right)^{1/2}. \qquad (5)$$

Here, α_2 and α_3 are the components of the tensor α along the principal axes of the ellipsoids, ϑ is the angle relative to these axes.

Since the oscillation periods corresponding to the directions $\vartheta_1 = 90°$ and $\vartheta_2 = 0°$ were measured, we were able to determine the values of α_2 and α_3 and, therefore, to calculate the components of the tensor α along the crystal axes.

The two other ellipsoids give the same projection in the yz plane. The corresponding formula, like the formulas for other planes, can be easily obtained from Eq. (3) and there is no need to calculate it.

It is not possible to determine the value of ϵ_f from the experiments on the geometrical resonance. However, if we use the data on the cyclotron masses, which were determined very accurately in [7], and the values of the momenta obtained in the present work, we can calculate all the constants of the spectrum in the quadratic approximation. These constants are listed in Table I. The quantities m_{ik} are the components of the tensor $1/\alpha$ in units of m_0. These were the parameters used in plotting the projections of the ellipsoids shown in Figs. 4—6.

It is evident from Table I that the areas S_1 and S_2 are in somewhat better agreement with the direct measurements of the extremal cross-sectional areas using the de Haas-van Alphen effect, than is the area S_3. It is quite likely that this is due to a slight departure of the form of the section S_3 from that of a perfect ellipse.

The density of electrons, calculated for the three ellipsoids, is

$$n_e = 8\pi p_1 p_2 p_3 / h^3 = (2.76 \pm 0.3)\cdot 10^{17}\ \text{cm}^{-3}.$$

This value is in good agreement with the hole density, calculated in [1]:

$$n_h = (2.76 \pm 0.2)\cdot 10^{17}\ \text{cm}^{-3}.$$

Using these parameters of the spectrum in the quadratic approximation, we can calculate all the values of the cyclotron masses and momenta of electrons. A comparison of the calculated values with the directly measured principal values of the masses [5,6] shows agreement to within 2—3%. The calculated and measured areas of the central cross sections are also in satisfactory agreement, but there is no dependence of the effective mass on the energy, which is contradictory to the findings of the magneto-optical investigations. [19]

Table I

Constants of spectrum	Present investigation	[1,2]	[5]	[9]	[10]	[19]
$\varepsilon_f \cdot 10^{14}$	2.75±0.5	2.8±0.1				
m_{xx}/m_0	0.006±0.0006	0.0052±0.0012	0.00709	0.0088	0.0062	0.00521
m_{yy}/m_0	1.22±0.12	1.5±0.3	1.71	1.8	1.3	1.2
m_{zz}/m_0	0.0246±0.0025	0.03±0.006	0.0305	0.023	0.017	0.0204
m_{yz}/m_0	−0.128±0.013	±0.16	0.176	±0.16	−0.085	−0.09
$S_1 \cdot 10^{42}$	1.31±0.1	1.34±0.05				
$S_2 \cdot 10^{42}$	13.1±1	14±1.5				
$S_3 \cdot 10^{42}$	18±1.5	22±1 19.5±1				

Table II

ε_f	m_{xx}/m_0	m_{yy}/m_0	m_{zz}/m_0	m_{yz}/m_0	Reference
$4{,}54\cdot10^{-14}$	0.00127	0.26	0.00523	−0.0271	Present study
$4{,}43\cdot10^{-14}$	0.00113	0.26	0.00443	−0.195	[19]

In estimating the principal parameters of the electron Fermi surface, we shall consider only the ellipsoidal nonquadratic approximation,[13,14] which allows for the energy dependence of the effective mass. In this case, the energy dispersion law is written as:

$$\varepsilon(1+\varepsilon/\varepsilon_0) = \mathbf{p}\alpha\mathbf{p}/2m_0. \qquad (6)$$

In this formula, α, the reciprocal mass tensor, has the same form as in Eq. (2). The masses depend on the energy as follows:

$$m_c = m_{c0}(1+2\varepsilon/\varepsilon_0), \qquad (7)$$

where m_{c0} is the mass at the bottom of the band.

The values of the constants obtained in this approximation are listed in Table II. The value $\epsilon_0 = 2.45 \times 10^{-14}$ was taken from the paper of Brown et al.[19]

The areas of the cross sections of the surface and the carrier densities were found to be the same as in the quadratic approximation. A comparison of the experimental data with the Abrikosov-Fal'kovskiĭ model cannot yet be carried out, because the constants in the equations of this model have not yet been calculated.

There is one more published model of the spectrum, and that is the nonellipsoidal and nonquadratic spectrum of bismuth.[11] A comparison with this model will not be made because we found no great deviations of the Fermi surface from the ellipsoidal shape.

The experimental investigation reported here does not yet give an unambiguous model of the spectrum which would explain all the characteristics of bismuth. However, it is evident that the Fermi surface consists of surfaces which differ very little from ellipsoids, both in the case of holes and electrons.

In conclusion, the author thanks É. A. Kaner, M. S. Khaĭkin, and L. A. Fal'kovskiĭ for valuable discussions, and O. G. Shevchenko for undertaking the purification of bismuth and the measurement of its resistance.

[1] Brandt, Dolgolenko, and Stupochenko, JETP **45**, 1319 (1963), Soviet Phys. JETP **18**, 904 (1964).

[2] N. B. Brandt and L. G. Lyubutina, JETP **47**, 1711 (1964), Soviet Phys. JETP **20**, 1150 (1965).

[3] D. N. Reneker, Phys. Rev. **115**, 303 (1959).

[4] E. P. Vol'skiĭ, JETP **43**, 1120 (1962), Soviet Phys. JETP **16**, 791 (1963).

[5] Yi Han Kao, Phys. Rev. **129**, 1122 (1963).

[6] G. E. Smith, Phys. Rev. Letters **9**, 487 (1962).

[7] Khaĭkin, Mina, and Édel'man, JETP **43**, 2063 (1962), Soviet Phys. JETP **16**, 1459 (1963).

[8] M. S. Khaĭkin and V. S. Édel'man, JETP **47**, 878 (1964), Soviet Phys. JETP 20, 587 (1965).

[9] Galt, Yager, Merritt, Cetlin, and Brailsford, Phys. Rev. **114**, 1396 (1959).

[10] Smith, Hebel, and Buchsbaum, Phys. Rev. **129**, 154 (1963).

[11] M. H. Cohen, Phys. Rev. **121**, 387 (1961).

[12] A. A. Abrikosov and L. A. Fal'kovskiĭ, JETP **43**, 1089 (1962), Soviet Phys. JETP **16**, 769 (1963).

[13] B. Lax, Bull. Am. Phys. Soc. **5**, (1960).

[14] B. Lax, Rev. Mod. Phys. **30**, 122 (1958).

[15] A. A. Galkin and A. P. Korolyuk, PTÉ No. 6, 99 (1960).

[16] V. L. Gurevich, JETP **37**, 71 (1959), Soviet Phys. JETP **10**, 51 (1960).

[17] A. A. Galkin and A. P. Korolyuk, JETP **36**, 1307 (1959), Soviet Phys. JETP **9**, 925 (1959).

[18] Smith, Barraf, and Rowell, Phys. Rev. **135**, A1118 (1964).

[19] Brown, Mavroides, and Lax, Phys. Rev. **129**, 2055 (1963).

Translated by A. Tybulewicz
129